The Transient Mass-Flow Adjustment of Heated Atmospheric Circulations

JAN PAEGLE[1]

National Center for Atmospheric Research,[2] Boulder, CO 80307

(Manuscript received 20 December 1977, in final form 18 May 1978)

ABSTRACT

The transient adjustment of the baroclinic structure of a warm core disturbance forced by heating is studied as an initial value problem. It is found that the divergent flow in convective regions adjusts on a time scale of a few hours, and the surrounding divergence field outward to about 2000 km adjusts on a time scale of about 1 day. This rapid adjustment is due to the outward radiation of gravity inertia waves. The adjustment is sufficiently rapid that diurnally periodic forcings produce divergence fields that are almost in phase, and in practically instantaneous equilibrium with the forcings.

In the case of latent heatings associated with local precipitation rates in excess of a few centimeters per day, the strongly anticyclonic upper tropospheric pressure field may render the balance equation non-elliptic. When they occur in the tropics, isolated events of this magnitude can produce cross-isobaric flows on the order of 1 m s^{-1} outward to beyond 2000 km. A plausible influence of these tropical flows upon midlatitudes is hypothesized, following the argument in a climatological study by Blackmon *et al.* (1977). The present results suggest that the mechanism in question can act on time scales as short as one or two days after the inception of a strong tropical disturbance.

1. Introduction

A variety of investigations have dealt with the adjustment of synoptic-scale flows to heating. Eliassen (1952) investigates slow thermally driven vortices. Charney and Eliassen (1964), Kuo (1965) and others study the generation of tropical storms through conditional instability of the second kind. Parameterization theories of Kuo (1965), Ooyama (1971) and Arakawa and Schubert (1974) represent attempts to couple the instantaneous rate of moist convective heating to various concurrent synoptic-scale measures of the atmospheric state.

These theories generally have a quasi-equilibrium hypothesis that limits the respective conclusions to heated circulations whose time scales are large with respect to certain adjustment times. In the instance of quasi-balanced circulations it is assumed that the time scale must be larger than that associated with geostrophic adjustment. In the case of parameterization theories, the time scale of destabilization is large with respect to the time scale of individual convective elements. It is therefore questionable whether such approaches may be appropriate for events in which heating commences and ceases abruptly and almost independently of any deep tropospheric circulation. Consequently, the theoretical studies have usually avoided such highly transient phenomena.

One purpose of this study is to describe the transient adjustment of heated flow within the context of a linearized, hydrostatic model in which the heating rate is pre-specified, and assumed to be strongest in the mid-troposphere. The assumption that the heating is independent of the generated flow may be valid only initially or for weak flow generation. However, in the absence of a reasonable cumulus parameterization theory for highly transient phenomena, it may be difficult to improve upon this significantly. The presumption of maximum heating in the mid-troposphere is qualitatively reasonable for rather deeply disturbed conditions.

These assumptions result in a governing equation analogous to the gravity inertia wave equation that arises for a discretely layered fluid (Section 2). Thus, this adjustment problem is formally analogous to the homogeneous problem first treated by Cahn (1945). Important generalizations are that the forcing appears as an inhomogeneity, and the adjusted steady-state has flow divergence as opposed to Cahn's non-divergent geostrophic steady state.

It is possible to obtain exact integral solutions, applying to unbounded domains, that can be evaluated by quadrature. This is described in Section 3. Sample solutions are described in Section 4. They illustrate that the adjustment to impulsive onset of steady localized heating produces a nearly steady state *divergence* field

[1] On leave from the Department of Meteorology, University of Utah, Salt Lake City 84112.

[2] The National Center for Atmospheric Research is sponsored by the National Science Foundation.

0022-4928/78/1678-1688$05.50

over the heated region on the time scale of a few hours, and an effectively steady state *divergence* outward to about 2000 km after about 1 day. This rapid adjustment appears to be due to the energy dispersion associated with the local nature of the forcing and rapid outward radiation of transient gravity waves produced by the impulse. Although the Coriolis parameter plays only a minor dispersive role, it is critically important for the existence of a large region of flow compensation that surrounds the heated area.

Section 5 investigates the limitations placed upon this approach due to linearization. It appears that although, in the vicinity of substantial heating, the total nonlinear flow may depart from the linear solution, the linear divergence solution is a reasonable simulation of the nonlinear case. It is suggested that upper divergent outflow from individual strong tropical disturbances may modify higher latitude flows.

2. Mathematical model

a. *Assumptions and equations*

The analysis is based upon the standard two-layer model of the atmosphere linearized about a resting basic state. Following the usual notation (e.g., Matsuno, 1966) the equations of motion and thermodynamics may be written

$$\frac{\partial \mathbf{V}_1}{\partial t}+f\mathbf{K}\times\mathbf{V}_1+\nabla\phi_1=0, \tag{1}$$

$$\frac{\partial \mathbf{V}_3}{\partial t}+f\mathbf{K}\times\mathbf{V}_3+\nabla\phi_3=0, \tag{2}$$

$$\frac{\partial}{\partial t}(\phi_3-\phi_1)+s\Delta p\omega_2=-RQ. \tag{3}$$

Here $(\mathbf{V}_1,\mathbf{V}_3)$ represent (upper, lower) tropospheric horizontal velocities, (ϕ_1,ϕ_3) are the respective geopotentials, s, defined as

$$s=\alpha\frac{\partial \ln\theta}{\partial p}, \tag{4}$$

is the stratification, ω_2 the vertical motion in the mid-troposphere, R the gas constant, f the Coriolis parameter, $\mathbf{K}$ the unit vertical vector, Δp is the pressure thickness of each of the two layers and Q a specified heating rate (°C s^{-1}) in the mid-troposphere.

In the present applications Δp will be 500 mb, so that levels (1,2,3) correspond to pressures (250,500,750) mb.

Values of Q on the order of 10°C day^{-1} will be taken in the mid-troposphere. Such heating rates occur only in association with precipitation rates on the order of 2 cm day^{-1}. The assumption that Q is independent of large scale ω is a reasonable first approximation in circumstances where the atmosphere can produce heavy precipitation, conditional to the availability of moisture, and where that availability is modulated rapidly and virtually independently of the heat-generated motion field. These conditions are typically met over many continental climates during the summer, and also in the tropics. Here, the rather strong ambient conditional instability is often released or suppressed by rapidly changing motions of the moist boundary layer that can be effectively decoupled from the deeper troposphere. Diurnal oscillations represent an important case having these characteristics. In other cases where Q is strongly dependent upon ω, this assumption is poor, but the results may still have "diagnostic" value.

Defining the vertical shear $\mathbf{V}_D$ and geopotential thickness ϕ_D as

$$\mathbf{V}_D=\mathbf{V}_1-\mathbf{V}_3, \tag{5}$$

$$\phi_D=\phi_1-\phi_3, \tag{6}$$

equations (1), (2) and (3) may be rewritten

$$\frac{\partial \mathbf{V}_D}{\partial t}+f\mathbf{K}\times\mathbf{V}_D+\nabla\phi_D=0, \tag{7}$$

$$\frac{\partial \phi_D}{\partial t}+(s\Delta p^2/2)\nabla\cdot\mathbf{V}_D=RQ. \tag{8}$$

Here, the continuity equation has been integrated to give approximately

$$\omega_2=-\nabla\cdot\mathbf{V}_1\Delta p=\nabla\cdot\mathbf{V}_3\Delta p \tag{9}$$

and ω is assumed to be zero at the top and bottom of the model.

Eqs. (7) and (8) can be combined into a single equation

$$\frac{\partial^2\nabla\cdot\mathbf{V}_D}{\partial t^2}+f^2\nabla\cdot\mathbf{V}_D-c^2\nabla^2(\nabla\cdot\mathbf{V}_D)=-R\nabla^2Q, \tag{10}$$

where

$$c=\pm(s\Delta p^2/2)^{\frac{1}{2}} \tag{11}$$

is assumed constant.

Eq. (10) governs the baroclinic structure of the divergence field of a heated disturbance. In the homogeneous (adiabatic) case, the solutions tend to a non-divergent geostrophic balance from initially unbalanced states, as in Cahn's (1945) barotropic case. It is clear that heating must modify this conclusion.

In subsequent sections only the divergence of the upper level will be displayed. Because of the vertical structure of the present model, the governing equation of this is

$$\frac{\partial^2 D}{\partial t^2}+f^2D-c^2\nabla^2D=-G_1, \tag{12}$$

where

$$\left.\begin{aligned} D &\equiv \nabla\cdot\mathbf{V}_1 \\ G_1 &\equiv R\mathbf{V}^2Q/2 \end{aligned}\right\}. \tag{13}$$

b. Implications of the assumptions

Subsequent sections will emphasize the evolution of the divergence field as given by the solution of (10). It is important to note that although the divergence field tends to a steady state, the same does not hold for the vorticity and temperature fields in the linear model with non-zero Coriolis parameter.

The vertical shear of the vorticity is governed by

$$\frac{\partial}{\partial t}(\mathbf{K}\cdot\nabla\times\mathbf{V}_D) = -f(\nabla\cdot\mathbf{V}_D). \tag{14}$$

Thus, the vorticity continues to change even after the divergence has attained a steady value. Since (7) implies thermal wind balance for the vorticity (for steady divergence), this implies that θ is changing also. This monotonic time change of both horizontal circulation and potential temperature for steady divergence are consequences of the continued energy input and lack of dissipation. These features also exist in heated quasi-geostrophic models of atmospheric motions.

It is useful to describe the linear cases because they admit closed solutions which, for the divergence field, are similar to those of the nonlinear equations. The exact solutions help illustrate the adjustment process. They suggest that the divergence field adjusts on a rather small time scale associated with the rapid dispersion of transient internal gravity waves, while the rotational field adjusts more slowly, particularly at large distances where the divergence is small.

3. Solutions

a. Steady state, no rotation

In the steady case with $f=0$, one solution of (12) is

$$D = RQ/(2c^2), \tag{15}$$

showing that divergence above heated flows varies inversely with the stratification. This conclusion holds approximately for more complicated cases as well.

b. Normal mode solution

Assuming a rectangular geometry, and a component of Q of the form

$$A_{k,l,\omega}e^{i(kx+ly+\omega t)}$$

gives a response $D_{k,l,\omega}$ in the same component of amplitude:

$$D_{k,l,\omega} = Rg(k^2+l^2)A_{k,l,\omega}/[(-\omega^2+f^2)+c^2(k^2+l^2)]. \tag{16}$$

Resonance can occur only if

$$c^2(k^2+l^2) = \omega^2 - f^2.$$

c. Initial value solutions

Although normal mode techniques may be used to simulate solutions to initial value problems, this is a tedious task for truly local disturbances in effectively unbounded domains, and may produce singularities at resonance. It is also possible to obtain closed solutions for such cases more explicitly. In the inhomogeneous case, Duhamel's principle [see Churchill, 1972, p. 270, Garabedian, 1964, p. 210 and Carslaw and Jaeger (1959) for other examples] is useful because such solutions to the homogeneous problem are known.

We consider first a homogeneous linear differential equation:

$$L(v) \equiv \frac{\partial^2 v}{\partial t^2} + \sum_j A_j \frac{\partial^2 v}{\partial x_j^2} - \beta v = 0, \tag{17}$$

with data assigned at $t=\tau$:

$$\left.\begin{aligned} v(\mathbf{x},t;\tau) &= F(\mathbf{x},\tau) = 0 \quad (\text{at } t=\tau) \\ \frac{\partial v}{\partial t}(\mathbf{x},t;\tau) &= G(\mathbf{x},\tau) \end{aligned}\right\}.$$

Here, t is time and $(x_1, x_2, \ldots)=\mathbf{x}$ is a point in space. Then, the Duhamel integral

$$u(\mathbf{x},t) = \int_0^t v(\mathbf{x},t;\tau)\,d\tau \tag{18}$$

will be the solution to the inhomogeneous equation

$$L(u) = G(\mathbf{x},t)$$

with homogeneous initial conditions.

The demonstration proceeds by operating on (18) with L, which gives

$$L[u(\mathbf{x},t)] = \frac{\partial v}{\partial t}(\mathbf{x},t;\tau) = G(\mathbf{x},t).$$

Therefore, the solution of the general inhomogeneous problem

$$L(u) = G_1(\mathbf{x},t)$$

is given by the τ integral (18) of those solutions of the homogeneous Eq. (17) for which $G_1(\mathbf{x},t)$ represents initial data on $\partial v/\partial t$ at $t=\tau$, while the initial data on v at $t=\tau$ is 0.

This approach is useful because initial value solutions to the homogeneous gravity inertia wave equation have been given for the one-dimensional problem by Cahn (1945) and for the two-dimensional case by Obukhov (1949) (see Phillips, 1963; Blumen, 1972). The complete solution of (12) satisfying the radiation condition

at large distance in the one-dimensional case (assuming no variation in y) is then

$$D(x,t)=\left\{\int_{x-ct}^{x+ct} G(\xi)J_0\{(f/c)[c^2t^2-(\xi-x)^2]^{\frac{1}{2}}\}d\xi + \frac{\partial}{\partial t}\int_{x-ct}^{x+ct} F(\xi)J_0\{(f/c)[c^2t^2-(\xi-x)^2]^{\frac{1}{2}}\}d\xi + \int_0^t d\tau\int_{x-c(t-\tau)}^{x+c(t-\tau)} G_1(\xi,\tau)J_0\{(f/c)[c^2(t-\tau)^2 - (\xi-x)^2]^{\frac{1}{2}}\}d\xi\right\}, \quad (19)$$

where

$$F(x)=D(x,\, t=0),$$

$$G(x)=\frac{\partial D}{\partial t}(x,\, t=0),$$

and J_0 is the zero-order Bessel function of the first kind.

In the two-dimensional case the solution is

$$D(x,y,t)=\frac{1}{2\pi c}\frac{\partial}{\partial t}\int_0^{2\pi}\int_0^{ct}\frac{F(x+\eta\cos\theta,\, y+\eta\sin\theta)}{S} \times\cos\left(\frac{fS}{c}\right)\eta d\eta d\theta+\frac{1}{2\pi c}\int_0^{2\pi}\int_0^{ct}\frac{G(x+\eta\cos\theta,\, y+\eta\sin\theta)}{S} \times\cos\left(\frac{fS}{c}\right)\eta d\eta d\theta+\int_0^t\frac{1}{2\pi c}\int_0^{2\pi}\int_0^{c(t-\tau)} \times\frac{G_1(x+\eta\cos\theta,\, y+\eta\sin\theta,\, \tau)}{S_1}\cos\left(\frac{fS_1}{c}\right)\eta d\eta d\theta d\tau, \quad (20)$$

where

$$F(x,y)\equiv D(x,\, y,\, t=0),$$

$$G(x,y)\equiv\left.\frac{\partial D}{\partial t}\right|_{t=0},$$

$$S\equiv(c^2t^2-\eta^2)^{\frac{1}{2}},$$

$$S_1\equiv[c^2(t-\tau)^2-\eta^2]^{\frac{1}{2}}.$$

The bounding cone of dependence and the geometrical interpretations of the symbols in (20) are depicted in Fig. 1.

The first two integrals of (19) and (20) represent solutions for the homogeneous case, obtained from Cahn (1945) (one-dimensional) and Obukhov (1949) (two-dimensional), while the third is the solution for the inhomogeneous case, obtained from the Duhamel integral.

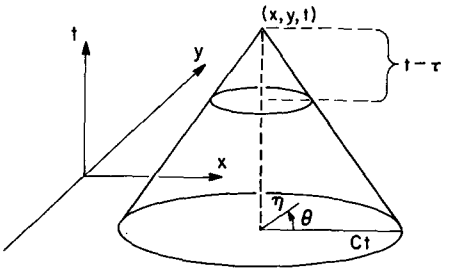

FIG. 1. Bounding cone of dependence and the geometrical interpretation of the symbols of Eq. (20).

With the exception of especially simple cases, analytical integration of (19) and (20) is difficult or impossible. Consequently, the solutions to be shown are all obtained by quadrature. One-dimensional Gaussian quadrature is used in each dimension, with the exception of the azimuthal integration in the two-dimensional case, where Simpson's rule is used. Up to six applications of ten-point quadrature are used in each dimension as required for resolution. Gaussian quadrature is not useful for integrands such as those in (20) with singularities. Therefore, the singularities at the edge of the bounding cone of dependence are removed by the variable transformation

$$y=-(a^2-\eta^2)^{\frac{1}{2}},$$

where

$$a^2=(ct)^2$$

in the first two integrals of (20) and

$$a^2=[c(t-\tau)]^2$$

in the third. The resulting integrals do not contain singularities.

4. Numerical examples

Particular one- and two-dimensional examples are illustrated in the present section. All start with zero divergence and zero divergence tendency ($F=0, G=0$) and the differences of the solutions are due to different forcings or latitudes.

a. One-dimensional impulsive heating

The following distribution of Q (°C day^{-1}) is assumed:

$$Q=\begin{cases}0, & \text{for all } x, \quad t<0\\ \{10\exp[-(kx)^2]-2\}, & t\geq 0.\end{cases} \quad (21)$$

We select $k = 1/(400$ km) to model heating within 500 km of the origin, peaking at $x=0$ at a rate of 8°C day^{-1} in the mid-troposphere. Assuming a vertical profile similar to that given by Newell *et al.* (1972, Table 7.3) for equatorial convection gives the column-averaged maximum heating rate of about 5°C day^{-1}, corresponding roughly to the latent heat release rate of about 1200 cal day^{-1} cm^{-2}. This corresponds to a maximum

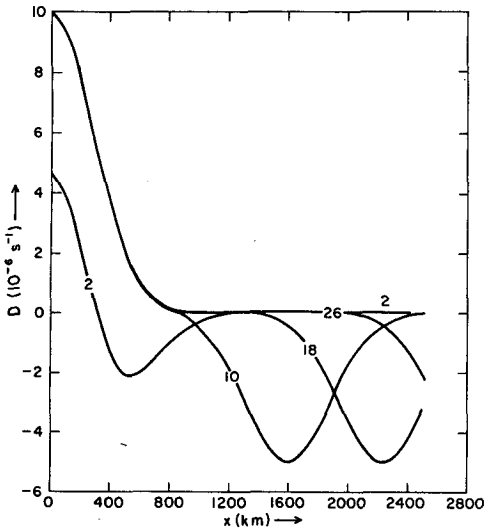

FIG. 2. One-dimensional divergence evolution for the case $k=1/(400\text{ km})$, $f=0$. Curve labels are in hours following heating onset (no initial divergence). Only the evolution for $x>0$ is shown since the solution is symmetric about $x=0$. See text for other details.

precipitation rate of about 2 cm day^{-1}. As $x\to\pm\infty$, Q becomes negative, asymptoting toward -2°C day^{-1} in the mid-troposphere. This is approximately the typical magnitude of longwave radiative cooling.

The impulsive onset simulated by (21) models a suddenly developing, and rather broad band of moderate precipitation. The parameter c is taken as 44 m s^{-1}, consistent with $\Delta p=500$ mb and a potential temperature lapse rate of 2.2°C km^{-1}. This lapse rate is between the standard lapse rate of 3.5°C km^{-1} and neutral stratification. It is sufficiently weak to be conditionally unstable in a moist atmosphere.

Solutions at equatorial and mid-latitudes are displayed in Figs. 2 and 3, respectively. The adjustment toward steady-state divergence occurs on a time scale of a few hours in the vicinity of the heating, but requires about a

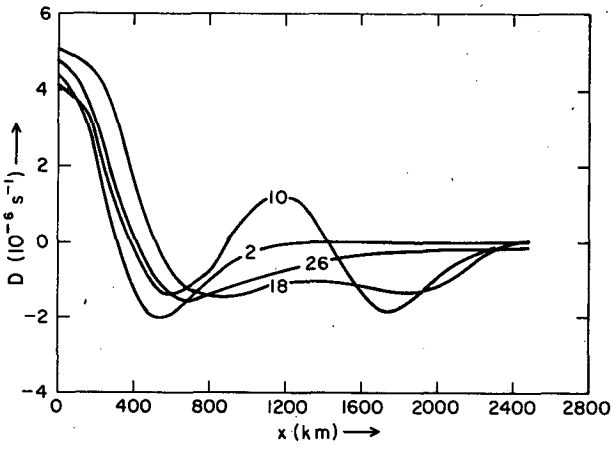

FIG. 3. As in Fig. 2, except for $f=10^{-4}$ s^{-1}.

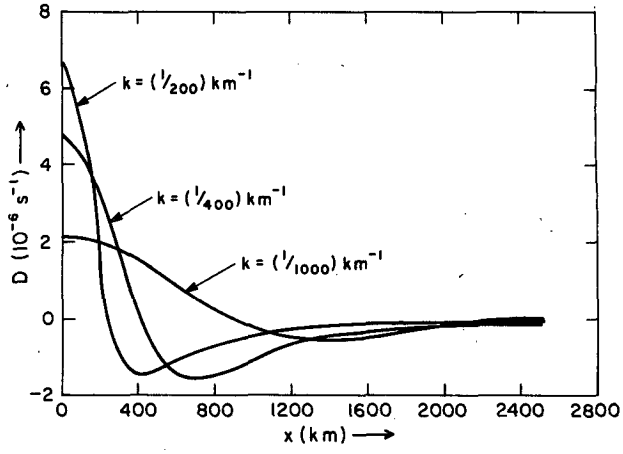

FIG. 4. One-dimensional steady-state divergence as a function of x for forcings of indicated scales, and $f=10^{-4}$ s^{-1}.

day or more at distances about 2000 km or further from the center of heating in mid-latitudes.

It is obvious that heating generates stronger divergent outflow in the tropics than in mid-latitudes. For the chosen scale, the implied vertical circulation is only about half as strong around 45° as at the equator.

The scale dependence of the adjusted steady state at about 45° latitude is depicted in Fig. 4. The heating is specified by (21) in all cases.

b. Two-dimensional impulsive heating

The distribution of Q in this case has the form

$$Q=\begin{cases}0, & \text{for all } r, \quad \text{for} \quad t<0\\ \{10\exp[-(kr)^2]-2\}, & t\geqslant 0\end{cases} \tag{22}$$

where r now represents radial distance from the center of heating. This two-dimensional case models a local

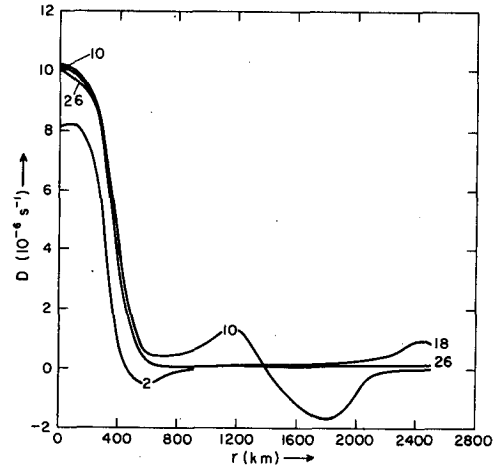

FIG. 5. Two-dimensional divergence evolution for the case $k=1/(400\text{ km})$, $f=0$. Curve labels are in hours following heating onset (no initial divergence). See text for further details.

source having the same maximum heating rate as the one-dimensional case. Figs. 5 and 6 illustrate the time evolutions of divergence for $f=0$ and $f=10^{-4}$ s^{-1}, respectively, for $k=(1/400)$ km^{-1}. The adjustment toward steady-state divergence in both cases again occurs within a few hours in the heated region and is almost complete outward to beyond 2500 km within one day. The transient gravity wave propagating outward from the center of the initial impulse damps much more markedly in Figs. 5 and 6 than in Figs. 2 and 3, due to the geometrical dispersive effect of two-dimensionality.

The scale dependence of the divergence displayed in Fig. 7 also suggests a stronger response for smaller scales.

c. Two-dimensional diurnally oscillating heating

The distribution of Q is now specified to be

$$Q=\begin{cases}0, & \text{for all } r, \quad t<0\\ \{10\cos(\omega t)\exp[-(kr)^2]-2\},\\ \quad \delta_{1n}\pi/2+n\pi/2-\pi<(\omega t)<n\pi/2, \quad n=1, 5, 9, \ldots\\ \{-10\cos(\omega t)\ (\exp[-(kr)^2]-1)-2\},\\ \quad n\pi/2-\pi<\omega t<n\pi/2, \quad n=3, 7, 11, \ldots\\ \quad \omega>0,\\ \quad \delta_{1n}=\begin{cases}1 & \text{if } n=1\\ 0 & \text{if } n\neq 1.\end{cases}\end{cases} \tag{23}$$

The solution to this problem becomes periodic as transients to the impulsive onset radiate outward. For the divergence, this occurs in about one day for the domains depicted in Figs. 8 and 9.

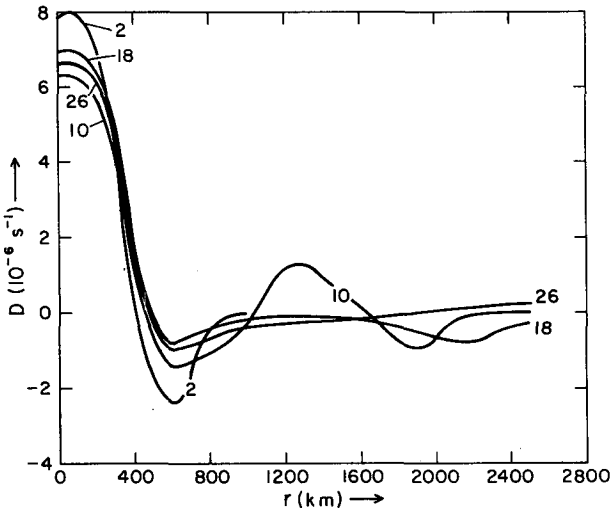

FIG. 6. As in Fig. 5, except for $f=10^{-4}$ s^{-1}.

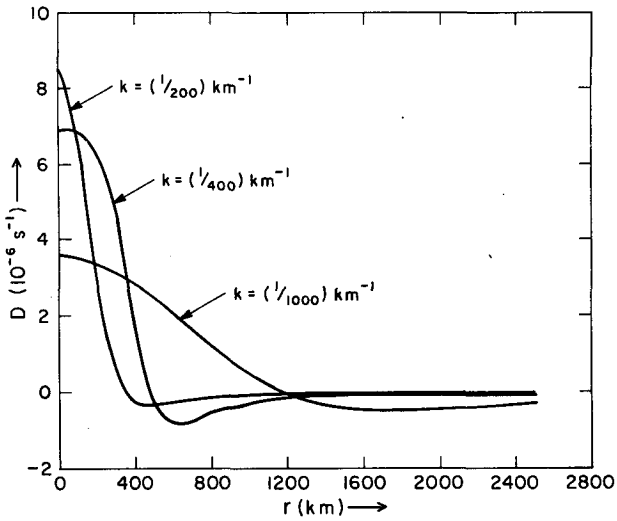

FIG. 7. Two-dimensional steady divergence as a function of r for forcings of indicated scales, and $f=10^{-4}$ s^{-1}.

Assuming $\omega=2\pi/24$ h, and $k=(1/400)$ km^{-1} simulates a diurnal oscillation in Q that might occur in areas where latent heating has a diurnal cycle. For the case that $f=10^{-4}$ s^{-1} (Fig. 8), the latitude is similar to the central Great Plains of the United States. Eq. (23) may then represent the diurnal oscillation of convective heating that is found there during the summer (Wallace, 1975), roughly one-half day out of phase with the convection over adjoining terrain. The particular heating rates imply a maximum precipitation of about $\frac{2}{3}$ cm in the course of a 12 h wet phase.

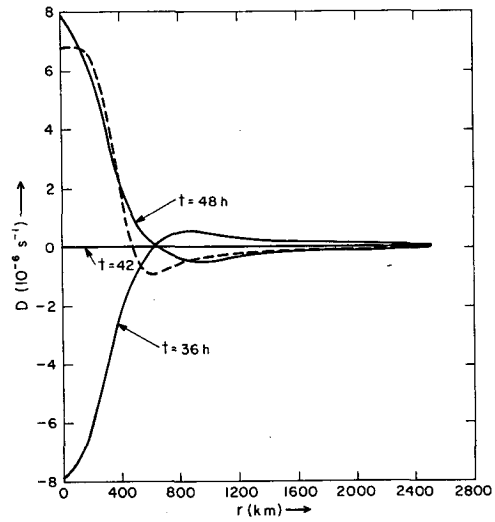

FIG. 8. Two-dimensional divergence as a function of t and r for $f=10^{-4}$ s^{-1} for diurnally oscillating forcings (solid curves). The solution at $t=42$ h coincides with the abscissa. The dashed curve is the steady-state solution corresponding to a steady forcing equal to that at 48 h. The 36 h steady result (not shown) is the negative of this.

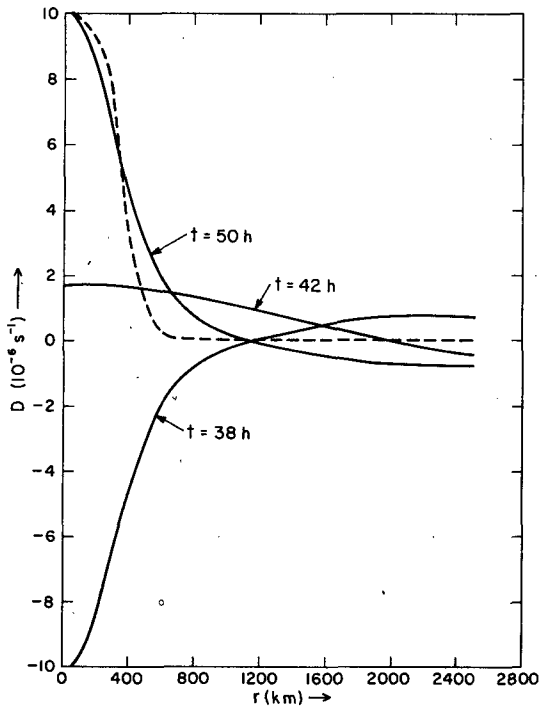

FIG. 9. As in Fig. 7 except for $f=0$. The upper and lower solid curves lag those of Fig. 7 by 2 h to correspond to the time of maximum response. The dashed curve is the steady solution corresponding to a steady forcing equal to that at 48 h.

The solutions at the times of maximum and minimum heating are rather similar to the steady-state solution corresponding to the forcing specified at these times. The fact that these solutions have somewhat larger magnitude than the steady-state solutions is a reflection of the amplified response suggested by (16) for $\omega^2>0$. However, their overall similarity to the corresponding steady solutions is an example of the remarkably rapid adjustment that the flow divergence in the present model makes to the heating.

The diurnally oscillating case for $f=0$ (Fig. 9) suggests a similar conclusion. It also indicates a slight broadening of scale, in accordance with (16), but no resonances because the present local forcing occurs in an infinite domain. This conclusion could be fundamentally different in normal mode treatments over periodic domains, that would have discrete spectra and possible resonances.

5. Nonlinearity

a. Equations

The linear solutions are likely to be valid only for small Rossby number. The importance of this assumption may be checked by returning to the nonlinear versions of (1)–(3). It is still assumed that the baroclinic disturbance has negligible horizontal flow and geopotential gradients at 500 mb. Although this appears to be a rather strong assumption, it is roughly consistent with the circulations composited by Reed and Johnson (1974) over the tropical western Pacific. This is also a useful assumption in order to isolate the modifications of the solutions due to nonlinearity.

The upper tropospheric temperature field T_1 may be approximated as

$$T_1=(\phi_1-\phi_2)/R, \tag{24}$$

where ϕ_2 is the mid-tropospheric geopotential.

For the radially symmetric case, the system governing the upper tropospheric flow is

$$\frac{\partial u}{\partial t}=-\left(u\frac{\partial u}{\partial r}+\omega\frac{\partial u}{\partial p}\right)+fv+\frac{v^2}{r}-\frac{\partial\phi_1}{\partial r}, \tag{25}$$

$$\frac{\partial v}{\partial t}=-\left(u\frac{\partial v}{\partial r}+\omega\frac{\partial v}{\partial p}\right)-uv/r-fu, \tag{26}$$

$$\frac{\partial\phi_1}{\partial t}=-u\frac{\partial\phi_1}{\partial r}+s\Delta p(\omega/2)+RQ/2. \tag{27}$$

Here (u,v,ω) are (radial, tengential, vertical) motions in the upper level, and (r,p) are (radial, vertical pressure) coordinates. It is assumed that only half of the total latent heating occurs in the upper layer, and that ϕ_2 is steady.

The following finite difference approximations are now used:

$$\omega=-\left(\frac{\partial u}{\partial r}+\frac{u}{r}\right)\Delta p/2, \tag{28}$$

$$\frac{\partial(u,v)}{\partial p}=-(u,v)/(\Delta p/2). \tag{29}$$

Substitution of (28), (29) into (25), (26), (27) gives

$$\frac{\partial u}{\partial t}-fv+\frac{\partial}{\partial r}(\phi_1)=-\left[\frac{\partial}{\partial r}(u^2)+\frac{u^2}{r}\right]+\frac{v^2}{r}, \tag{30}$$

$$\frac{\partial v}{\partial t}+fu=-\frac{\partial}{\partial r}(uv)-2uv/r, \tag{31}$$

$$\frac{\partial\phi_1}{\partial t}+\left(\frac{\partial u}{\partial r}+\frac{u}{r}\right)(s\Delta p^2/4)-RQ/2=-u\frac{\partial\phi_1}{\partial r}, \tag{32}$$

The right-hand sides of these represent the nonlinearities.

Linearized versions of (30)–(32) would lead to (12) with

$$c=\pm(s\Delta p^2/4)^{\frac{1}{2}},$$

instead of

$$c=\pm(s\Delta p^2/2)^{\frac{1}{2}}$$

as in (11). The difference is due to the finer vertical pressure differencing used presently. This resolves a shorter vertical mode than that implied in the original

two-layer model, resulting in slower horizontal propagation. If the stratification is maintained as in the previous examples, the amplitude of the response in D almost doubles as in the simpler solution (15), while the adjustment time increases by about 40% because of smaller c.

In the examples to be shown s will be taken to be twice its previous value, giving the same c value as before.

Eqs. (30), (31), (32) can be solved numerically. This is done using a simplified Adams Bashforth scheme that has second order accuracy in time. The grid size is 50 km, the time step 75 s, and the integration extends radially outward to 5000 km. Standard centered space differencing is used, and the numerical scheme is checked by comparison with a leapfrog approach that uses a horizontal staggering of variables suggested by Arakawa and Mesinger (1976) for geostrophic adjustment. These comparisons, as well as comparisons of linear numerical solutions with the previously discussed linear analytical solutions, are in good agreement, lending reliability to the present numerical calculation.

Fig. 10 illustrates the solution at 28 h (when the divergence and u are practically steady to beyond 2400 km) for the same case as shown in the linear solution in Fig. 6. The maximum vorticity in this case is 3.6×10^{-5} s^{-1}, and the ratio of this to the Coriolis parameter indicates a Rossby number of order 1/3 for this heating rate.

Linear numerical solutions of (30), (31) and (32) are shown for comparison. These solutions are very close to the linear analytic results. It is quite clear that at mid-latitudes the effect of nonlinearity upon the final divergence is small for the presently studied heating rates. The transient adjustment (not shown) is also rather similar to the linear solutions of Fig. 6.

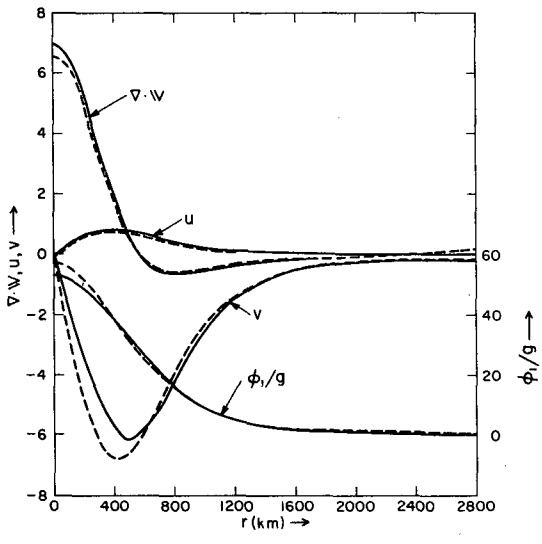

FIG. 10. Solution of $\nabla\cdot\mathbf{V}$ (10^{-6} s^{-1}), u (m s^{-1}), v (m s^{-1}), ϕ_1/g (m) for the two-dimensional case at $t=28$ h. Solid curves are from nonlinear equations (30), (31), (32) for the same case as in Fig. 6. The dashed curves are the predictions from a linear solution as explained in the text.

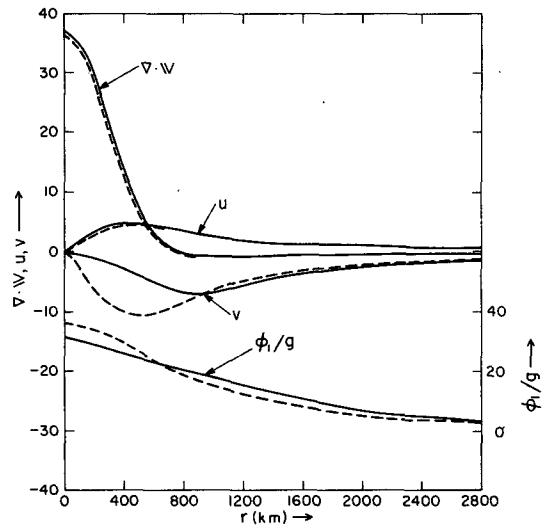

FIG. 11. As in Fig. 10 except at 10°N, and a heating rate that is four times as strong.

b. Heating and strongly nongradient flow

MacDonald (1977) and Paegle and Paegle (1976b) have described actual warm core systems for which the upper tropospheric flow is quasi-irrotational with respect to space, but strongly divergent. The Rossby number is then order 1 and the heating must be several times greater than that given by (22) in order to achieve this in the present model.

Fig. 11 displays solutions at 10°N, 28 h after the onset of heating that is four times as strong as given by (22). The maximum implied precipitation rate is 10 cm day^{-1} at $r=0$. The implied precipitation rate averaged over the region $r<400$ km is about 3 cm day^{-1} (corresponding to heating of about 10°C day^{-1}). This might represent a strongly convective circulation in the vicinity of the ITCZ. The upper level divergence is almost 4×10^{-5} s^{-1}, suggesting a Rossby number in excess of 1. Nevertheless, a linear numerical solution gives practically the same flow divergence profile.

This again suggests that the modifications due to advection are not very important for the simulation of flow divergence in the present model, although they are important for the vorticity and temperature. The flow shown in Fig. 11 is sufficiently nonlinear for the balance equation to be non-elliptic (e.g., Paegle and Paegle, 1974) within about 500 km of the center of heating, where

$$2\nabla^2(\phi_1)+f^2<0.$$

Paegle and Paegle (1974), (1976b) and (1978) have argued that quasi-steady divergence out of pressure fields for which the nondivergent balance equation is non-elliptic may be estimated directly from the pressure

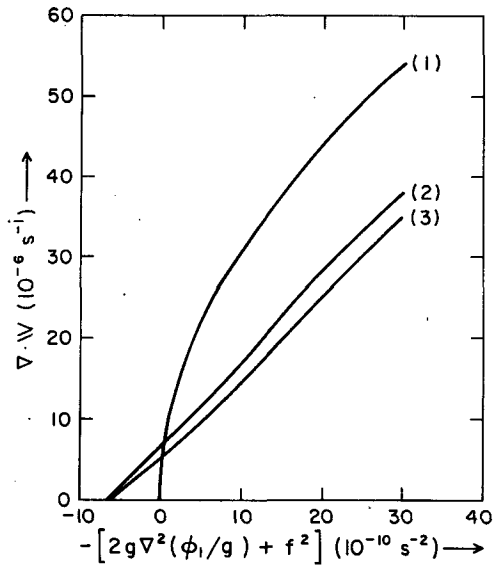

FIG. 12. Curve 1, divergence as a function of $2\nabla^2(\phi_1)+f^2$: from frictionless non-elliptic estimate as in Paegle and Paegle (1974); curve 2, from frictional non-elliptic estimate as in Paegle and Paegle (1978); curve 3, numerical solution from Eqs. (30), (31) and (32) from the case of Fig. 11.

field. The most recent of these studies (1978) includes a drag formulation of friction to simulate vertical mixing of vorticity, while the earlier (1974) and (1976) studies are frictionless.

Those diagnoses of the divergence as a function of

$$-[2\nabla^2(\phi_1)+f^2]$$

are compared in Fig. 12 with the present numerical results. The latter are averaged over the region $r<400$ km to represent a synoptic scale that includes the most intense heating. The drag coefficient in the frictional non-elliptic case (following Paegle and Paegle, 1978) is equal to 2.5×10^{-5} s^{-1}. In unpublished data investigations we have found that such a magnitude is necessary to account for a reasonable acceleration-force balance at 200 mb during Phase III of the GATE experiment.

The diagnostic estimates based upon our earlier studies of non-elliptic pressure fields neglect thermodynamics, tilting terms and inhomogeneities in the forcing field. The simple analytical solution indicated in the frictional non-elliptic case is nevertheless similar to the solution of the more complete case described in this study. Because of the different dynamics in these cases, the close agreement may be partly circumstantial, and detailed agreement should not be expected generally.

The present numerical solutions produce about half the divergence of the frictionless non-elliptic estimates over much of the non-elliptic range of Fig. 12. This ratio is similar to the ratio of observed outflows from heated regions to the diagnosed frictionless non-elliptic estimates computed by Paegle and Paegle (1976a).

Such comparisons may support the hypothesis that much observed upper level divergence may in fact be associated with pressure fields generated by such strong heating that the standard balance equation is non-elliptic.

If the latter conjecture is correct, then it is useful to obtain reasonable diagnostic mass-flow relations in these cases. This may be particularly important for initialization of tropical forecast models containing strongly convective features, and possibly for much larger scales as well.

Fig. 11 suggests that cross-isobaric flow on the order of 1 m s^{-1} exists to distances on the order of 2000 km from a strong localized disturbance in the tropics. Thus, the effect of such a disturbance may extend to latitudes of the subtropical jet stream, where zonal flow accelerations on the order of 5 m s^{-1} day^{-1} may be produced. The implied production of the vertical shear between the upper and lower troposphere is twice this magnitude. Blackmon *et al.* (1977) suggest that upper tropospheric cross-isobaric flow of magnitude 1–2 m s^{-1} may be important for intensifications of both the jet stream and (indirectly) the baroclinic waves in storm tracks over the western Pacific and the United States.

The present results do not prove the implied association between strong latent heat releases in the tropics and significant energy sources for the subtropical jet stream. However, if this effect does exist, then the solutions suggest that a single strong tropical disturbance may begin to influence higher latitudes on the remarkably short time scale of 1 or 2 days. If these speculations can be verified this would suggest the importance of local tropical disturbances even in short-range prediction of large-scale flows of mid-latitudes.

6. Conclusions

The principal conclusion is that deep atmospheric flow divergence adjusts to heating on rather short time scales (on the order of a day or less). One reason for this is that the deep gravity waves associated with the adjustment have high phase speeds, and their transients radiate away rapidly. Equivalently, the hydrostatic pressure field is strongly responsive for deep motions, and an efficient mass-flow adjustment occurs for the presently studied vertical structures. It may be noted that this is not the case for shallow motions (e.g., Bolin, 1953).

Inclusion of the feedback effects of the generated flow upon the latent heat release is beyond the scope of the present study. However, the fact that the present one-way adjustment to heating occurs so rapidly may support a tentative conclusion that quasi-steady hypotheses may actually apply reasonably well, even for diurnally periodic time scales. The feedback should be quantitatively significant, since the vertical velocity is on the order of 2–3 cm s^{-1} in most of the specific examples. Such vertical motions could significantly increase low-level moisture influxes, and may amplify

the final response. However, the convergence implied in the present mid-latitude examples (about 10^{-5} s^{-1}) is still smaller than that which seems to accompany diurnal boundary layer fluctuations over the United States (Paegle, 1978). Consequently, the actual triggering mechanism of the convection may not be dominated by the generated flows in these cases.

For adiabatic motions, the Rossby radius of deformation λ $(=c/f)$ is an important parameter (e.g., Washington, 1964; Cahn, 1945; Obukhov, 1949); λ is on the order of 400 km in the present mid-latitude examples. Scales smaller than λ are characterized by a divergence evolution that is similar to the non-rotating case, and is rather responsive to the heating, while the response for scales larger than λ is reduced.

It may be demonstrated that solutions (19), (20) possess nonzero area integrals of divergence over the infinite domain in the absence of rotation ($f=0$). However, all rotating linear cases that tend to a steady state and for which the solutions and forcing damp at least as fast as r^{-a} for large r and positive a, have zero area integrated divergence over the infinite domain. This can be shown by an area integration of (12), application of the divergence theorem, and taking the limit $r \to \infty$. This situation includes as special cases solutions to localized forcings that satisfy Sommerfeld's (1949) radiation condition (damping as $r^{-\frac{1}{2}}$). Therefore, total flow compensation may be expected in rotating flows. Solution (20) and Fig. 7 suggest that for heatings having a horizontal scale on the order of λ or less, flow divergence may be expected outward to distances of order λ and compensating convergence from about $\pi\lambda/2$ to about $3\pi\lambda/2$.

The solutions indicate that almost total compensation occurs over this area, and that the compensating convergence and related subsidence are about an order of magnitude weaker than in the central region. This suggests that the influence of locally heated disturbances in mid-latitudes is effectively limited to distances on the order of 2000 km, while heatings within the tropics may have an impact outward to larger distances.

The rotational flow component (v) changes rather slowly (in proportion to fu in a linear problem). Thus, the rotational component of the heat-driven circulation adjusts toward the steady-state value more slowly than the divergent part, particularly at radial distances beyond 1000 km. To the extent that tropical heating is relevant, the generation and maintenance of strong subtropical jet streams may therefore be favored in those areas that lie poleward of heavy and persistent tropical convective regions. It would be of interest to ascertain the degree of dependence of the climatologically strongest 200 mb cross-isobaric flow, as well as the strongest jet stream generation in the western Pacific upon the proximity of the heavy winter monsoon of the tropical western Pacific. We are pursuing both data and more complete model investigations of this question.

Acknowledgments. I wish to acknowledge Professor A. Arakawa for first describing to me the prototype equations for the adjustment of a baroclinic disturbance. I would also like to thank Dr. A. Kasahara and Dr. D. Stevens for useful comments and for helping me to improve the clarity of the manuscript. Part of this research was supported by the National Science Foundation under Grant ATM-77-17349.

REFERENCES

Arakawa, A., and W. Schubert, 1974: Interaction of a cumulus cloud ensemble with the large-scale environment. Part I. *J. Atmos. Sci.*, **31**, 674–701.

——, and F. Mesinger, 1976: Numerical methods used in atmospheric models. *GARP Publ. Ser.*, No. 17, 648 pp.

Blackmon, M., J. M. Wallace, N-Ch Lau and S. L. Mullen, 1977: An observational study of the Northern Hemisphere wintertime circulation. *J. Atmos. Sci.*, **7**, 1040–1053.

Blumen, W., 1972: Geostrophic adjustment. *Rev. Geophys. Space Phys.*, **10**, 485–528.

Bolin, B., 1953: The adjustment of a non-balanced velocity field towards geostrophic equilibrium in a stratified fluid. *Tellus*, **5**, 373–385.

Cahn, A., 1945: An investigation of the free oscillations of a simple current system. *J. Meteor.*, **2**, 113–119.

Carslaw, H. C., and J. C. Jaeger, 1959: *Conduction of Heat in Solids*. Clarendon Press, 510 pp.

Charney, J. G., and A. Eliassen, 1964: On the growth of the hurricane depression. *J. Atmos. Sci.*, **21**, 68–75.

Churchill, R. V., 1972: *Operational Mathematics*. McGraw-Hill, 481 pp.

Eliassen, A., 1952: Slow thermally or frictionally controlled meridional circulations in a circular vortex. *Astrophys. Norv.*, **5**, 19–60.

Garabedian, P. R., 1964: *Partial Differential Equations*. Wiley, 672 pp.

Kuo, H. L., 1965: On formation and intensification of tropical cyclones through latent heat release by cumulus convection. *J. Atmos. Sci.*, **22**, 40–63.

MacDonald, A. E., 1977: On a type of strongly divergent steady state. *Mon. Wea. Rev.*, **105**, 771–785.

Matsuno, T., 1966: Quasi-geostrophic motions in the equatorial area. *J. Meteor. Soc. Japan*, **44**, 25–42.

Newell, R. E., J. W. Kidson, D. G. Vincent and G. J. Boer, 1972: *The General Circulation of the Tropical Atmosphere and Interactions with Extratropical Latitudes*, Vol. 2, The MIT Press, 371 pp.

Obukhov, A., 1949: On the question of geostrophic wind. *Izv. Akad. Nauk SSSR, Ser. Geogra. Geofis.*, **13**, 231–306.

Ooyama, K., 1971: A theory for the parameterization of cumulus convention. *J. Meteor. Soc. Japan*, **49**, Special Issue, 744–756.

Paegle, J., 1978: A linearized analysis of diurnal boundary layer convergence over the topography of the United States. *Mon. Wea. Rev.*, **106**, 492–502.

——, and J. N. Paegle, 1974: An efficient and accurate approximation to the balance equation with application to non-elliptic data. *Mon. Wea. Rev.*, **102**, 838–846.

——, and J. N. Paegle, 1976a: On geopotential data and ellipticity of the balance equation: A data study. *Mon. Wea. Rev.*, **104**, 1277–1286.

Paegle, J. N., and J. Paegle, 1976b: On the realizability of strongly

divergent supergradient flows. *J. Atmos. Sci.*, **33**, 2300–2307.
——, and J. Paegle, 1978: Frictional effects in strongly divergent flows. *J. Atmos. Sci.* (in press).
Phillips, N. A., 1963: Geostrophic motion. *Rev. Geophys.*, **6**, No. 2, 123–176.
Reed, R. J., and R. H. Johnson, 1974: The vorticity budget of synoptic scale wave disturbances in the tropical western Pacific. *J. Atmos. Sci.*, **31**, 1784–1790.
Sommerfeld, A., 1949: *Partial Differential Equations*. Academic Press, 333 pp.
Wallace, J. M., 1975: Diurnal variations in precipitation and thunderstorm frequency over the conterminous United States. *Mon. Wea. Rev.*, **103**, 406–419.
Washington, W. M., 1964: A note on the adjustment towards geostrophic equilibrium in a simple fluid system. *Tellus*, **16**, 530–534.